

## Electronic Supporting Information

Electrochemical hydrogen evolution reaction boosted by constructing Ru nanoparticles assembled as a shell over semimetal Te nanorods surface in acid electrolyte

Xudong Yang, Zhixin Zhao, Xu Yu and Ligang Feng \*

School of Chemistry and Chemical Engineering, Yangzhou University, Yangzhou 225002, P.R. China.

Email: ligang.feng@yzu.edu.cn; fenglg11@gmail.com (L Feng\*)

## Experimental methods

### Chemicals

All chemicals are purchased and used without further purification. Ruthenium chloride hydrate ( $\text{RuCl}_3 \cdot x\text{H}_2\text{O}$ ), Tellurium dioxide ( $\text{TeO}_2$ ) and Ethylene glycol ( $\text{C}_2\text{H}_6\text{O}_2$  AR) are purchased from Shanghai Aladdin Bio-Chem Technology Co., LTD. L-Ascorbic acid is purchased from Shanghai Macklin Biochemical Co., Ltd. Potassium hydroxide (KOH AR) is purchased from Sinopharm Chemical Reagent Co., Ltd. Polyvinylpyrrolidone (Mw=40000) (PVP) is obtained from Energy Chemical. Vulcan XC-72 carbon black is bought from the Cabot Co. Milli-Q water is used throughout the experiments.

### Synthesis of Te@Ru nanorods

The synthesis of Te@Ru catalysts consists of two steps: (1) fabricating Te nanorods and (2) fabricating Te@Ru catalysts through solvothermal treatment in ethylene glycol.

In the first step, 0.168 g  $\text{TeO}_2$  and 0.168 g KOH are added into a beaker and dissolved in 30 mL of ethylene glycol under vigorous magnetic stirring at 85°C to form a homogeneous solution. After dissolving 0.1 g PVP in the solution, 0.45 g L-Ascorbic acid is added. The obtained solution is transferred into the Teflon-lined stainless steel with a volume capacity of 50 mL, sealed and reacted at 150°C for 6 h. Finally, the Te nanorods are precipitated using acetone, cleaned with Milli-Q and dried overnight in vacuum at 60°C.

In the second step, 0.025 g Te nanorods obtained above are added into 50 mL ethylene glycol and stirred for 20 min, followed by the addition of 0.4 g PVP and  $\text{RuCl}_3$  aqueous solution (Ru: 19.4 mg/mL) with different molar ratios of Ru/Te, namely, 0.5, 0.6, 0.7. It is stirring for 30 min until forming a homogeneous solution, then the obtained solution is transferred into a Teflon-lined stainless steel autoclave with a capacity of 100 mL, sealed, and reacted at 160°C for 6 h. Finally, the dark products are separated and collected by centrifugation with acetone, cleaned with Milli-Q and dried overnight in vacuum at 60°C. The catalysts are denoted as Te@Ru-n (n is precursor molar ratios of Ru/Te). Ru nanoparticles are prepared following the same procedure with only adding ethylene glycol and L-Ascorbic acid.

### Characterization

The sample is characterized on Bruker D8 advance X-ray diffraction (XRD) with Cu K $\alpha$  radiation. The morphology is examined with a FEI Sirion-200 scanning electron microscope (SEM) and a transmission electron microscope (TEM) operating at 200 Kv. X-ray detector spectrum (EDS) images are obtained on a TECNAI G2 F30 transmission electron microscope (acceleration voltage: 300 kV). X-ray photoelectron spectroscopy (XPS) measurement are carried on an ECSALAB250Xi

spectrometer with an Al K $\alpha$  radiation source. Raman scattering is performed on a Jasco Raman spectrometer with excitation by 532 nm laser light.

## Catalytic activity test

### (1) Electrochemical measurements

All the electrochemical measurements are carried out with a Bio-Logic VSP electrochemical workstation (Bio-Logic Co., France) and a conventional three-electrode system. The working electrode is a glassy carbon electrode (3 mm diameter, 0.07 cm<sup>-2</sup>). The graphite rod and the saturated calomel electrode (SCE) serve as a counter and a reference electrode, respectively. All potentials are converted and referred to the reversible hydrogen electrode (RHE),  $E(\text{RHE}) = E(\text{SCE}) + 0.059 \text{ pH} + 0.242 \text{ V}$  and the ohmic potential drop loss caused by the electrode resistance is subtracted unless stated otherwise. For the electrocatalysis experiment, a drop of commercial Pt/C or the prepared catalyst solution is placed on the surface of the glassy carbon electrode and dried at the room temperature. The Te@Ru/C catalyst suspensions are prepared by dispersing 4 mg catalyst and 1 mg carbon black in 1 mL solution containing 0.95 mL ethanol and 0.05 mL 5 wt.% Nafion with sonication for 1 h to form a homogeneous ink. The Te@Ru catalyst suspensions with different molar ratios are also prepared in the same way except without adding XC-72 carbon black. Then 5 $\mu$ L of the catalyst ink is pipetted and dropped onto a pre-cleaned working electrode. The glassy carbon electrode is polished, thoroughly cleaned with alumina slurry of 0.05  $\mu$ m and finally dried at the room temperature before using. For HER experiment, the linear sweep voltammograms (LSV) and cyclic voltammograms (CV) are measured at 5 mV s<sup>-1</sup> in 0.5 M H<sub>2</sub>SO<sub>4</sub> solution.

### (2) Tafel analysis

For the Tafel equation,  $\eta = a + b \log(j)$ , where  $\eta$  is the overpotential and  $j$  is the current density.

### (3) ECSA and Turnover frequency (TOF) calculations

To estimate the effective surface areas of catalysts, we measure the capacitances of double layer at the solid-liquid interface by cyclic voltammograms (CVs) collected in the region of 0.142-0.242 V vs. RHE.

The electrochemical active surface area is calculated using the following formula:<sup>1</sup>

$A_{\text{ECSA}} = C_{\text{dl}} / C_s$  ( $C_s$  is specific capacitance = 0.04 mF cm<sup>-2</sup> in 0.5 M H<sub>2</sub>SO<sub>4</sub>), the specific activity is obtained by normalizing the apparent current to  $A_{\text{ECSA}}$ .

To calculate the TOF, we used the following formula:<sup>2</sup>

$$\text{TOF} = (j \times 3.12 \times 10^{15}) / (\# \text{ active sites} \times A_{\text{ECSA}})$$

### (4) Electrochemical impedance measurements

The ohmic resistance used for iR-correction is obtained from electrochemical impedance spectroscopy measurements with frequencies ranging from 1000 kHz to 10 mHz with an amplitude of 5 mV.

#### (5) Stability test and Chronoamperometry measurements

The dynamical stability is tested for 1000 cycles at the constant scan rate of 50 mV s<sup>-1</sup>. After 1000 cycles, the stable polarization curve is recorded for comparison with the initial curve. To estimate the stability of the catalysts, the chronoamperometry (CA) is performed in 0.5 M H<sub>2</sub>SO<sub>4</sub> solution at a potential of -0.086 V vs. RHE for 10 h.

#### (6) Faradaic yield tests

The working electrode is prepared by drop-casting catalyst suspension on the glassy carbon electrode with the surface area of 0.07 cm<sup>2</sup>. A constant potential of -0.086 V vs.RHE is applied on the electrode and the evolved gas is recorded continually. Thus, the faradaic yield is calculated from the ratio of the recorded gas volume to the theoretical gas volume during the charge passed through the electrode.

$$\text{Faradaic yield} = \frac{V_{\text{experimental}}}{V_{\text{theoretical}}} = \frac{V_{\text{experimental}}}{\frac{1}{2} \times \frac{Q}{F} \times V_m}$$

where Q is the charge passed through the electrode, F is Faraday constant (96485.3 C/mol), the number 2 means 2 mole electrons per mole H<sub>2</sub>, the number 1 means 1 mole H<sub>2</sub>, V<sub>m</sub> is molar volume of gas (24.5 L mol<sup>-1</sup>, 298 K, 101 KPa).

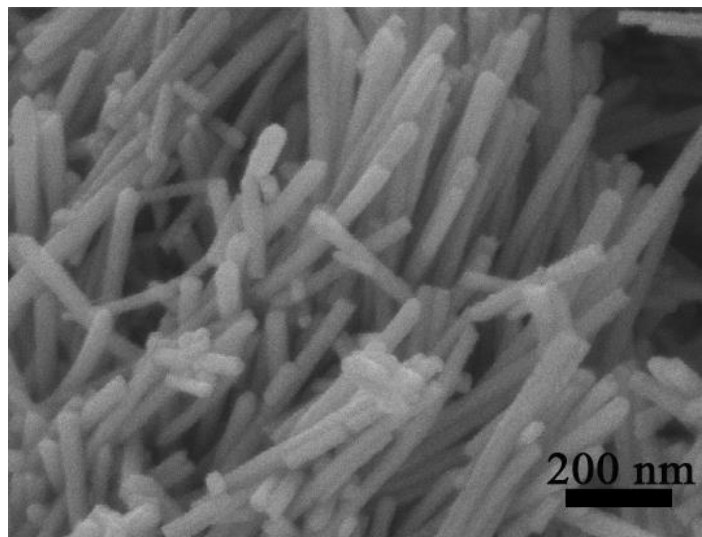


**Fig. S1** SEM image of as-prepared Te nanorods.

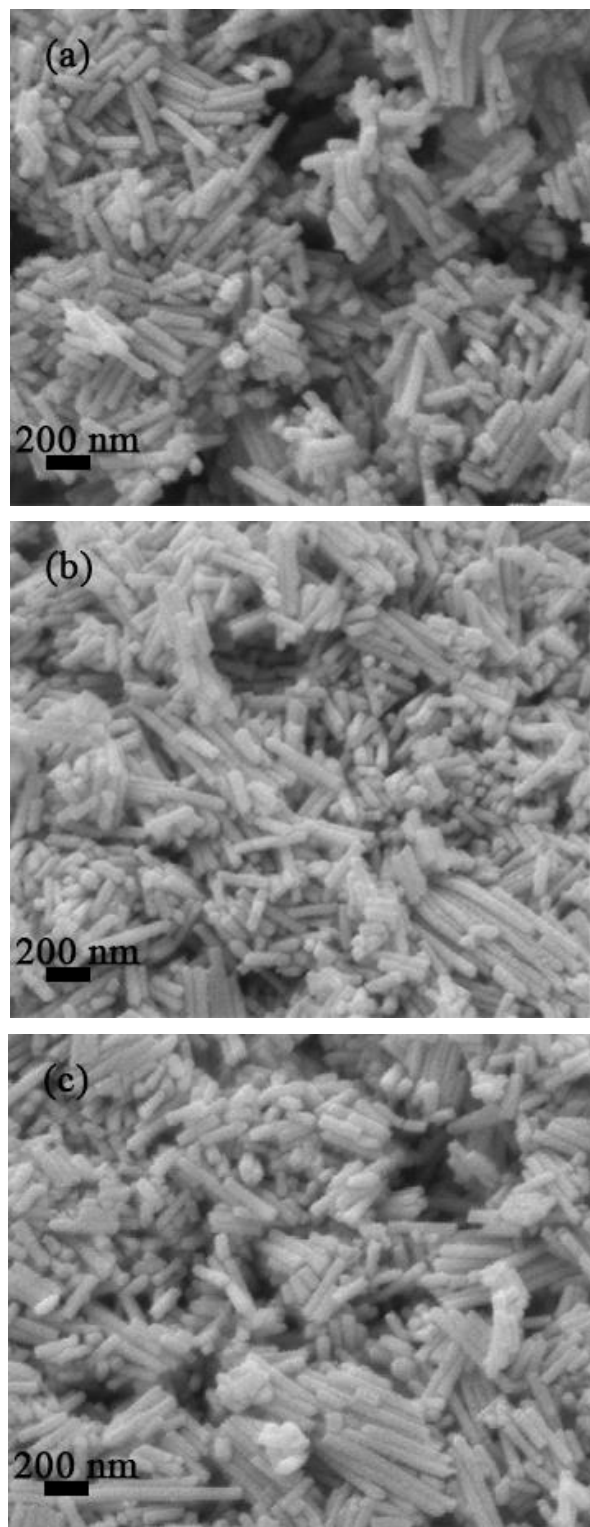


**Fig. S2** SEM images of Te@Ru-0.5 (a), Te@Ru-0.6 (b) and Te@Ru-0.7 catalysts (c).

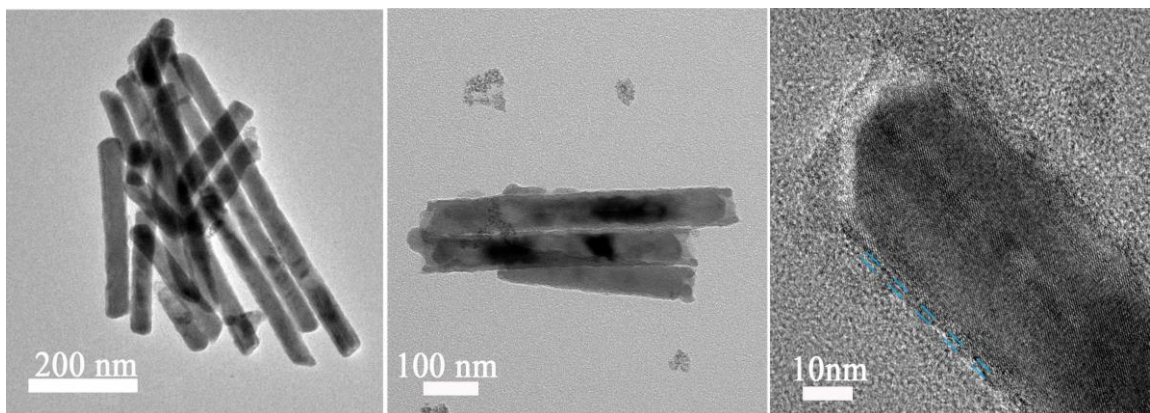


**Fig. S3a** TEM images Te@Ru-0.5 catalyst.

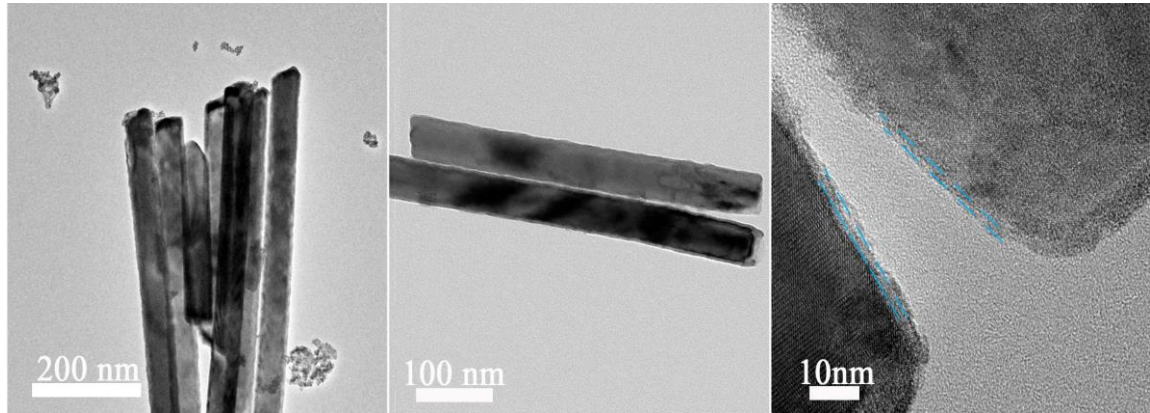


**Fig. S3b** TEM images Te@Ru-0.7 catalyst.

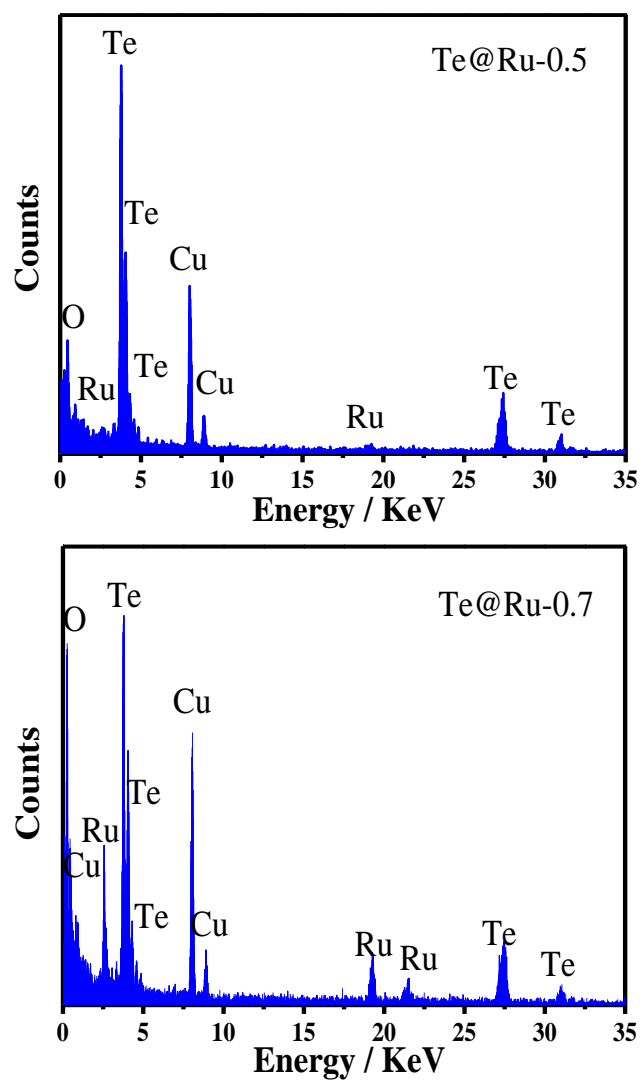


**Fig. S4** The EDS composition for Te@Ru-0.5 and Te@Ru-0.7 catalysts.

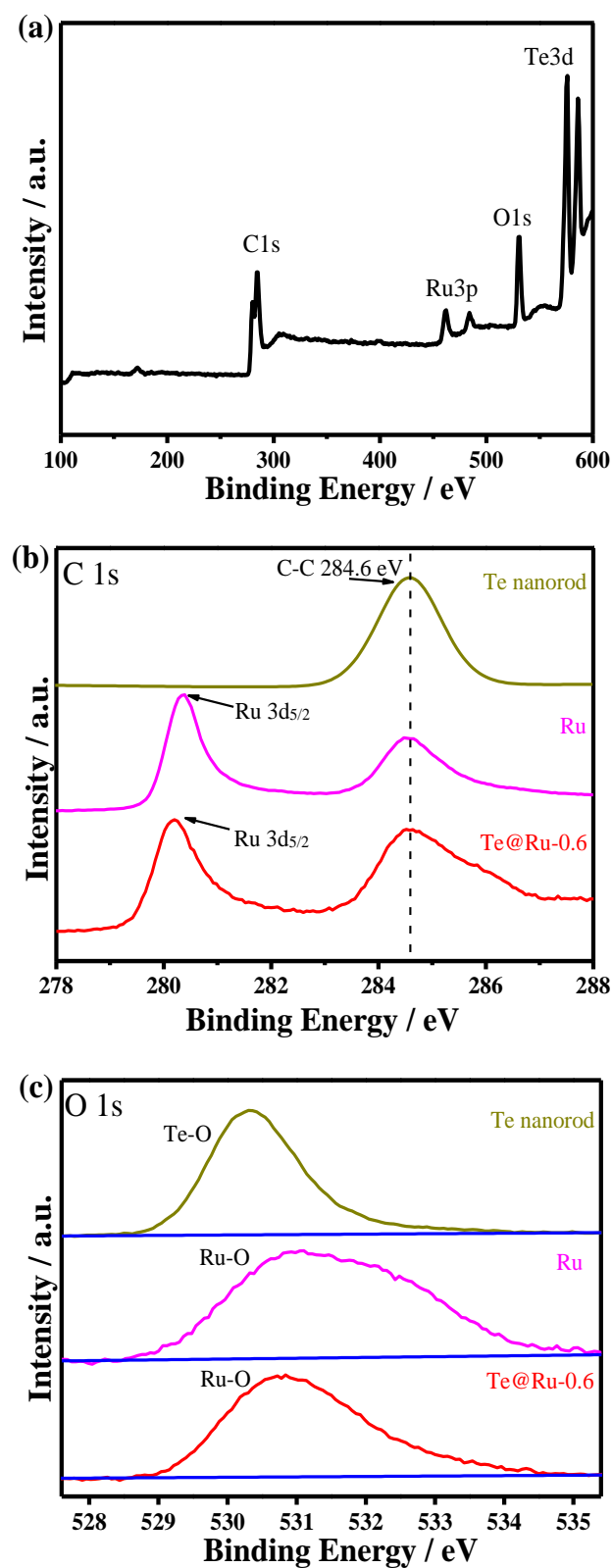


**Fig. S5** The whole XPS spectrum of Te@Ru-0.6 catalyst (a), high-resolution XPS spectra of C1s (b) and O 1s (c) for Te@Ru-0.6, Ru and Te nanorod, respectively.

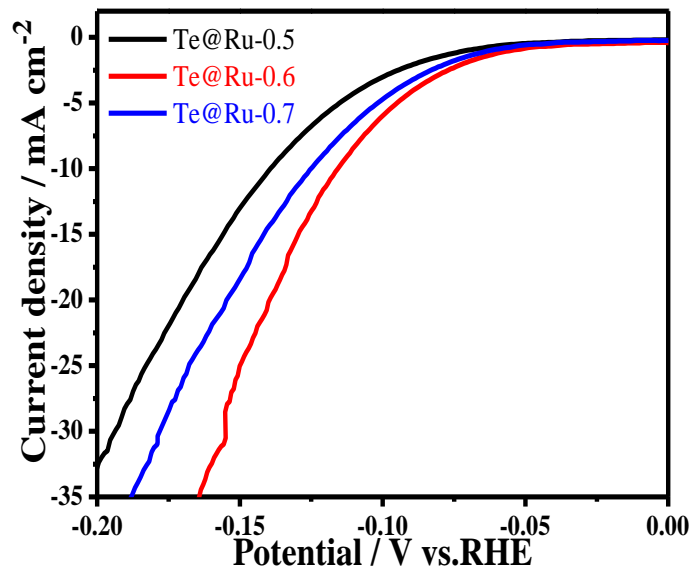


**Fig. S6** Polarization curves of the Te@Ru-0.5, Te@Ru-0.6 and Te@Ru-0.7 for HER in 0.5 M H<sub>2</sub>SO<sub>4</sub> solution.

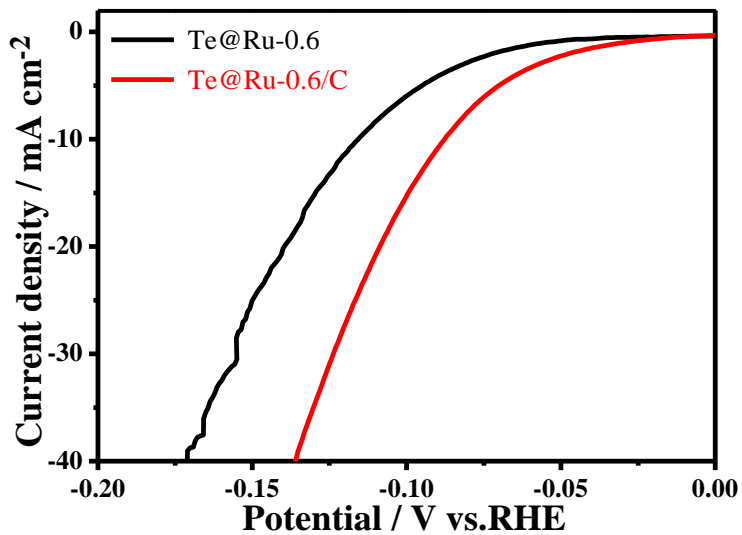


**Fig. S7** Polarization curves of the Te@Ru-0.6 and Te@Ru-0.6/C for HER in 0.5 M  $\text{H}_2\text{SO}_4$  solution.

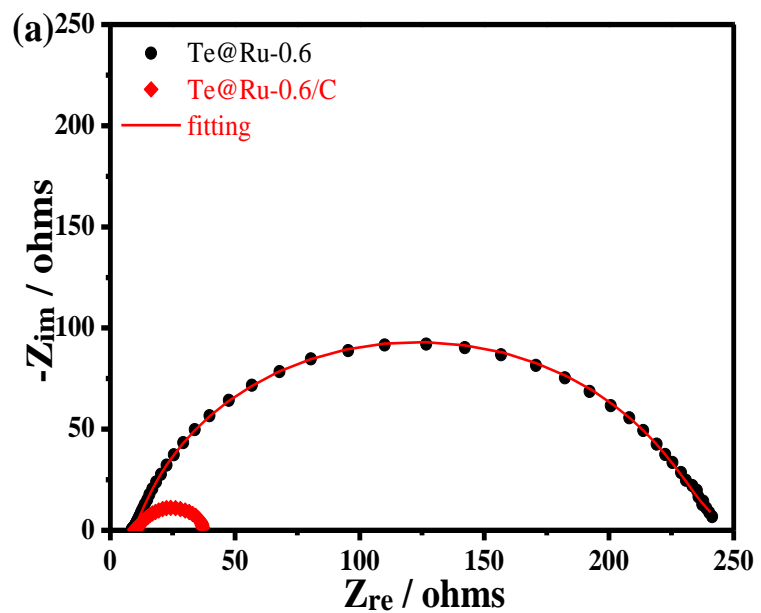


**Fig. S8a** Nyquist plots of Te@Ru-0.6 and Te@Ru-0.6/C at potential of -0.088 V vs. RHE in 0.5M H<sub>2</sub>SO<sub>4</sub> solution.

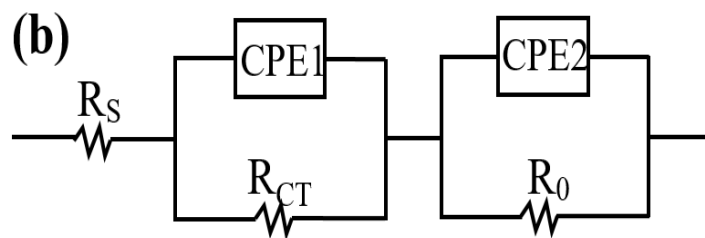


**Fig. S8b** The equivalent circuit of the electrochemical process, in which  $R_s$  is the solution resistance,  $R_{ct}$  and  $R_0$  represent charge transfer resistance and adsorption resistance respectively. The constant phase angle element (CPE) represents the double layer capacitance of a solid electrode in the real-world situation.

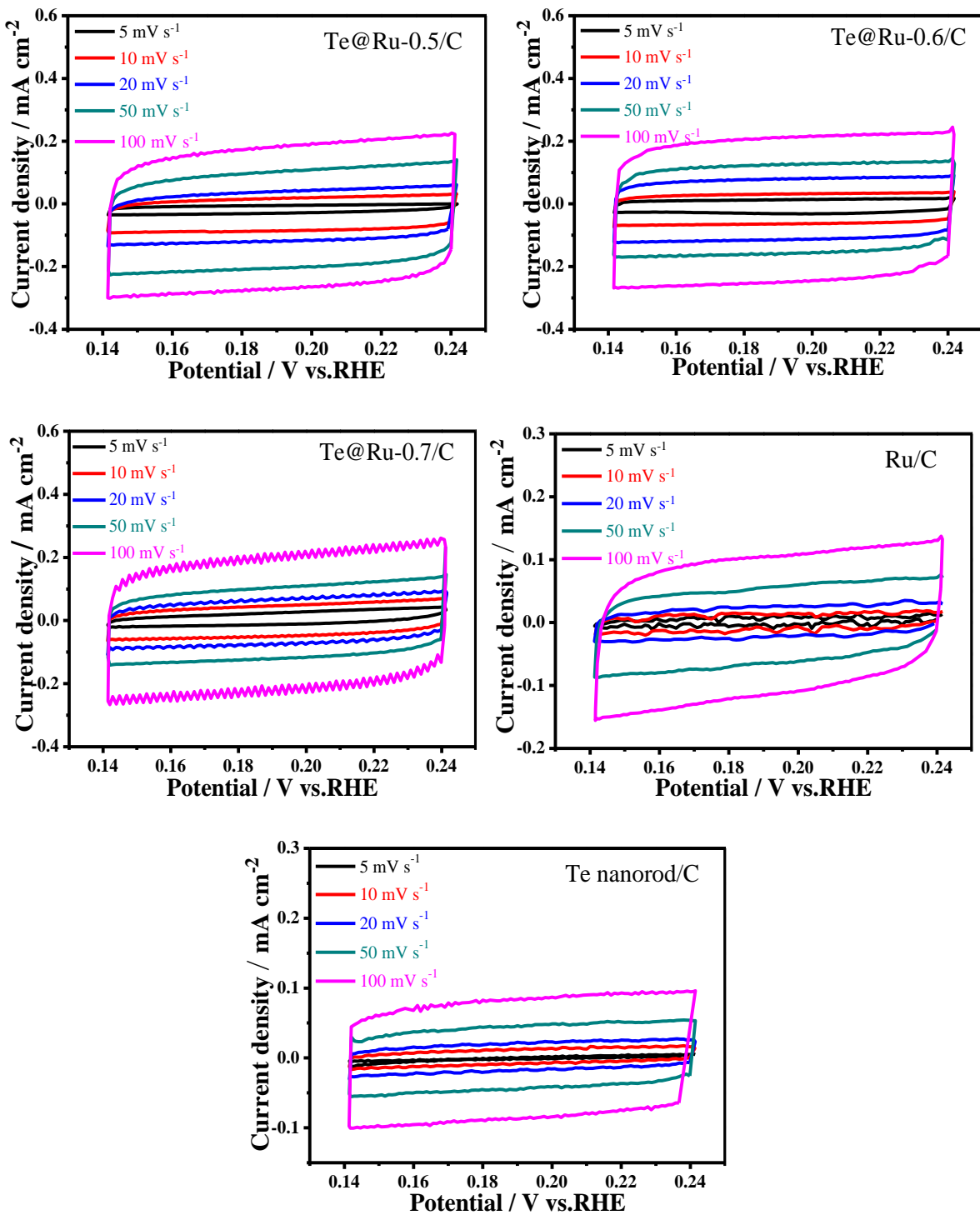


**Fig. S9a** Cyclic voltammograms for the double layer capacitance from 0.142 to 0.242 V for Te@Ru-0.5/C, Te@Ru-0.6/C and Te@Ru-0.7/C, Ru/C and Te nanorod/C in 0.5 M  $\text{H}_2\text{SO}_4$  solution.

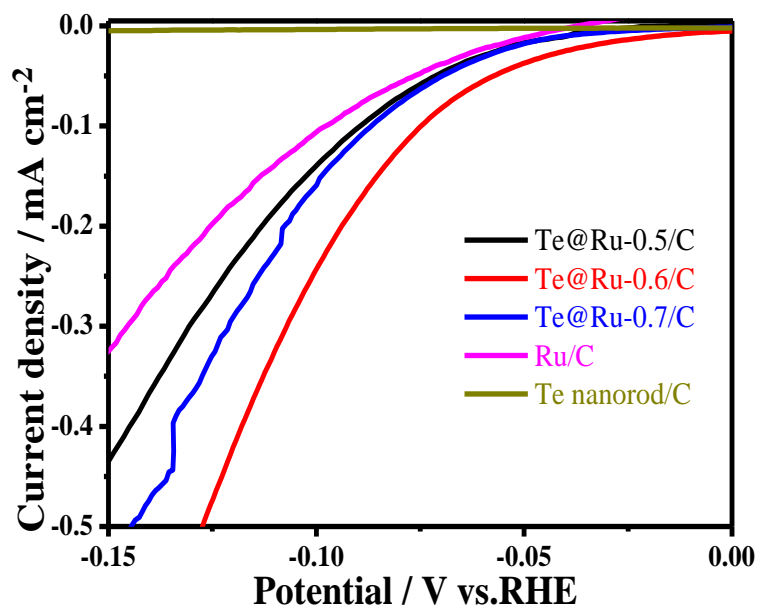


**Fig. S9b** Specific activity of Te@Ru/C with different molar ratios, Ru/C and Te nanorod/C at 5 mV s<sup>-1</sup> in 0.5 M H<sub>2</sub>SO<sub>4</sub>.

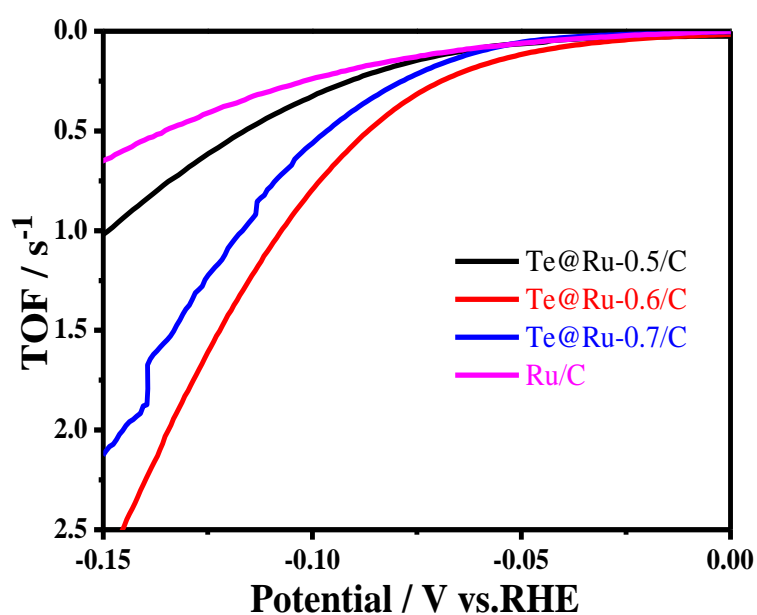


**Fig. S9c** TOF value of Te@Ru/C with different molar ratios and Ru/C as a function of overpotentials.

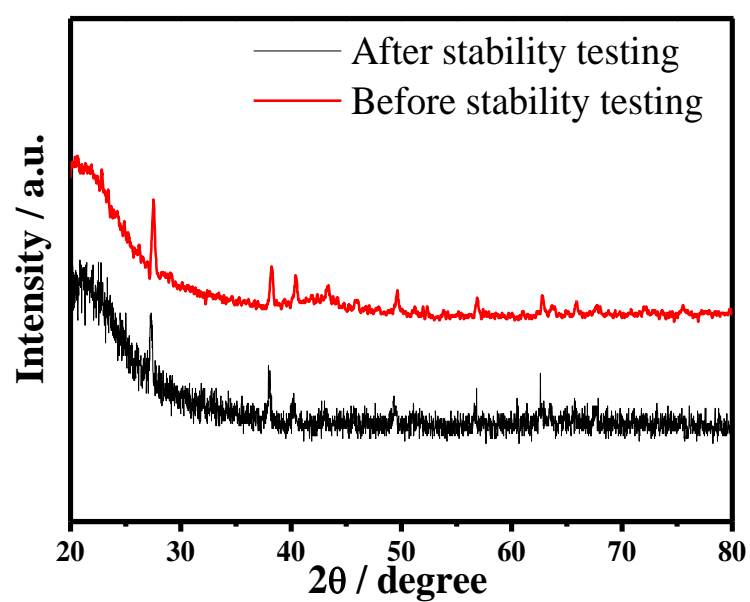


**Fig. S10** XRD patterns for Te@Ru-0.6 catalysts before and after long-term stability test in 0.5 M H<sub>2</sub>SO<sub>4</sub> solution.

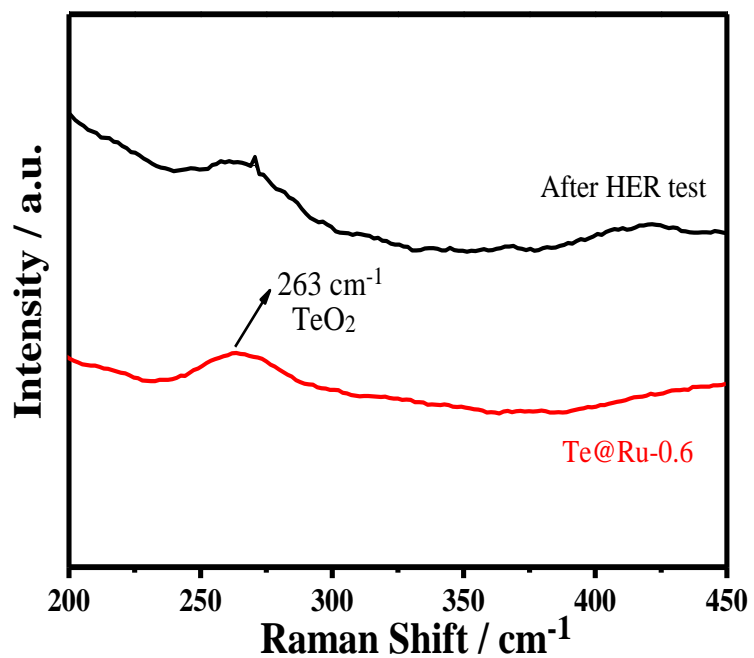


**Fig. S11** Raman spectra for Te@Ru-0.6 catalysts before and after long-term stability test in 0.5 M H<sub>2</sub>SO<sub>4</sub> solution.

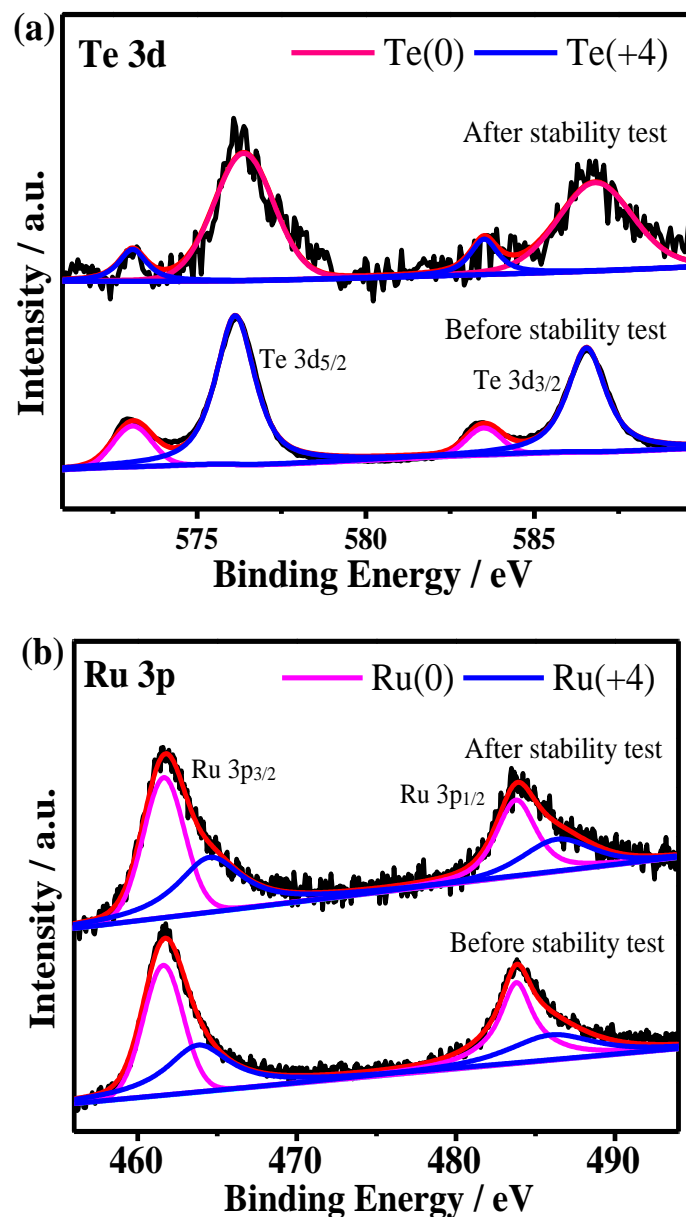


**Fig. S12** XPS spectra of Te 3d (a) and Ru 3p (b) for Te@Ru-0.6 catalysts after long-term stability test in 0.5 M H<sub>2</sub>SO<sub>4</sub> solution.

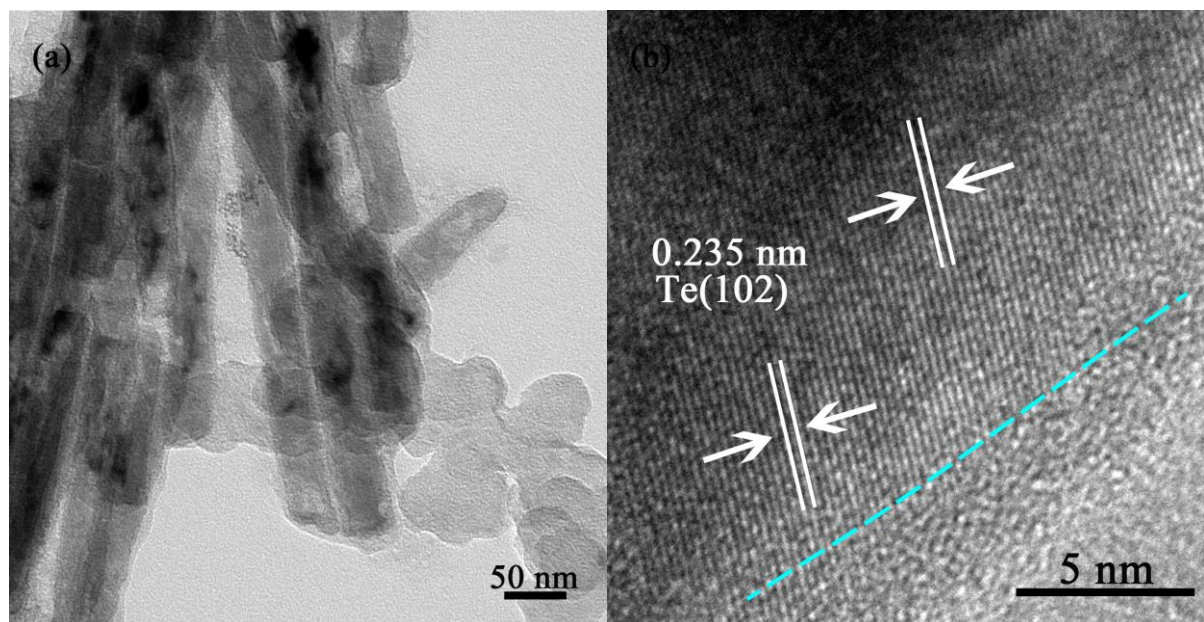


**Fig. S13** TEM image (a) and HRTEM image (b) of Te@Ru-0.6/C after long-term stability tests.

**Table S1.** Ru/Te molar ratios based on the EDS and ICP-OES data of Te@Ru catalysts with different molar ratios, respectively.

Catalysts	EDS	ICP-OES
Te@Ru-0.5	0.46±0.03	0.45±0.02
Te@Ru-0.6	0.58±0.03	0.57±0.02
Te@Ru-0.7	0.68±0.03	0.65±0.02

**Table S2.** Binding energies of the Te 3d<sub>5/2</sub> and Te 3d<sub>3/2</sub> components for Te@Ru-0.6 and Te nanorod.

Catalysts	Te 3d <sub>5/2</sub>		Te 3d <sub>3/2</sub>		Relatively content of Te(+4)
	Peak	Binding energy / eV	Peak	Binding energy / eV	
Te@Ru-0.6	Te(0)	573.0	Te(0)	583.4	85%
	Te(+4)	576.3	Te(+4)	586.7	
Te nanorod	Te(0)	572.9	Te(0)	583.3	67%
	Te(+4)	576.2	Te(+4)	586.6	

**Table S3** Binding energies of the Ru 3p<sub>3/2</sub> and Ru 3p<sub>1/2</sub> components for Te@Ru-0.6 and Ru.

Catalysts	Ru 3p <sub>3/2</sub>		Ru 3p <sub>1/2</sub>		Ru(0)/Ru(+4)
	Peak	Binding energy / eV	Peak	Binding energy / eV	
Te@Ru-0.6	Ru(0)	461.6	Ru(0)	483.8	1.5
	Ru(+4)	463.8	Ru(+4)	486.0	
Ru	Ru(0)	461.7	Ru(0)	483.9	1.3
	Ru(+4)	463.9	Ru(+4)	486.1	

**Table S4** The comparison of some representative HER electrocatalysts in an acidic electrolyte.

Materials	Electrode substrate	Overpotential (mV)	Reference
		@ 10 mA cm <sup>-2</sup>	
Te@Ru-0.6/C	GCE	86	This work
Ru/C	GCE	130	This work
1D-RuO <sub>2</sub> -CNx	GCE	93	3
Ni-Mo-S nanosheet	GCE	200	4
Co-NG	GCE	147	5
Co-NRCNTs	GCE	260	6
MoP <sub>2</sub> NPs	Mo plate	143	7
Ru/CN	GCRDE	127	8
Mo-Mo <sub>2</sub> C-0.077	GCE	150	9
Ni <sub>2</sub> P nanoparticles	GCE	125	10
C <sub>3</sub> N <sub>4</sub> -Ru-F	GCE	140	11
Cu <sub>2-x</sub> S@Ru NPs	GCE	129	12
1T-WS <sub>2</sub> nanosheets	GCE	230	13
Pt-MoS <sub>2</sub>	GCE	139	13
RuP <sub>2</sub> nanoparticles	GCE	129	14
MoS <sub>2</sub> /carbon	GCE	159	15
Mn <sub>2</sub> C/CNT-GR	GCE	130	16
MoS <sub>0.94</sub> P <sub>0.53</sub>	GCE	150	17
Ru-MoS <sub>2</sub>	GCE	300	18

\*GCE: glassy carbon electrode; GCRDE: glassy carbon rotating disk electrode.

**Table S5** EIS fitting parameters from equivalent circuits for different catalyst samples.

Samples	R <sub>s</sub> /Ω	R <sub>ct</sub> /Ω	CPE1/S s <sup>-n</sup>	R <sub>0</sub> /Ω	CPE2/S s <sup>-n</sup>
Te@Ru-0.5/C	8.54	119.50	3.75E-4	74.96	8.47E-3
Te@Ru-0.6/C	8.32	83.55	3.13E-4	34.44	5.52E-3
Te@Ru-0.7/C	8.61	102.61	3.01E-4	41.02	9.35E-3
Ru/C	8.93	180.20	8.72E-4	103.15	9.01E-3
Te nanorod/C	11.90	623.51	8.35E-4	231.31	9.54E-3

**Table S6** Double layer capacitance ( $C_{dl}$ ) and electrochemical surface areas (ECSA) for Te@Ru-n/C with different molar ratios, Ru/C, and Te nanorod/C.

Samples	Te@Ru-0.5/C	Te@Ru-0.6/C	Te@Ru-0.7/C	Ru/C	Te nanorod/C
$C_{dl}$ / mF	0.14	0.21	0.16	0.12	0.05
ECSA / cm <sup>2</sup>	3.50	5.25	4.00	2.99	1.25

## Reference

1. Z. Pu, Q. Liu, A. M. Asiri and X. Sun, *ACS applied materials & interfaces*, 2014, **6**, 21874-21879.
2. L. Zhang, X. Ren, X. Guo, Z. Liu, A. M. Asiri, B. Li, L. Chen and X. Sun, *Inorganic Chemistry*, 2018, **57**, 548-552.
3. T. Bhowmik, M. K. Kundu and S. Barman, *ACS Appl. Mater. Interfaces*, 2016, **8**, 28678-28688.
4. J. Miao, F. X. Xiao, H. B. Yang, S. Y. Khoo, J. Chen, Z. Fan, Y. Y. Hsu, H. M. Chen, H. Zhang and B. Liu, *Sci. Adv.*, 2015, **1**, e1500259.
5. H. Fei, J. Dong, M. J. Arellano-Jimenez, G. Ye, N. Dong Kim, E. L. Samuel, Z. Peng, Z. Zhu, F. Qin, J. Bao, M. J. Yacaman, P. M. Ajayan, D. Chen and J. M. Tour, *Nat. Commun.*, 2015, **6**, 8668.
6. X. Zou, X. Huang, A. Goswami, R. Silva, B. R. Sathe, E. Mikmekova and T. Asefa, *Angew. Chem., Int. Ed.*, 2014, **53**, 4372-4376.
7. Z. Pu, I. Saana Amiinu, M. Wang, Y. Yang and S. Mu, *Nanoscale*, 2016, **8**, 8500-8504.
8. J. Mahmood, F. Li, S. M. Jung, M. S. Okyay, I. Ahmad, S. J. Kim, N. Park, H. Y. Jeong and J. B. Baek, *Nat. Nanotechnol.*, 2017, **12**, 441-446.
9. J. Dong, Q. Wu, C. P. Huang, W. F. Yao and Q. J. Xu, *J. Mater. Chem. A*, 2018, **6**, 10028-10035.
10. L. Feng, H. Vrubel, M. Bensimon and X. Hu, *Phys. Chem. Chem. Phys.*, 2014, **16**, 5917-5921.
11. Y. Peng, B. Lu, L. Chen, N. Wang, J. E. Lu, Y. Ping and S. Chen, *Journal of Materials Chemistry A*, 2017, **5**, 18261-18269.
12. D. Yoon, J. Lee, B. Seo, B. Kim, H. Baik, S. H. Joo and K. Lee, *Small*, 2017, **13**, 1700052.
13. A. Ambrosi, Z. Sofer and M. Pumera, *Chemical communications*, 2015, **51**, 8450-8453.
14. Z. Pu, I. S. Amiinu, Z. Kou, W. Li and S. Mu, *Angew. Chem., Int. Ed.*, 2017, 11717-11722.
15. L. Yang, W. Zhou, J. Lu, D. Hou, Y. Ke, G. Li, Z. Tang, X. Kang and S. Chen, *Nano Energy*, 2016, **22**, 490-498.
16. D. H. Youn, S. Han, J. Y. Kim, J. Y. Kim, H. Park, S. H. Choi and J. S. Lee, *ACS nano*, 2014, **8**, 5164-5173.
17. R. Ye, P. del Angel-Vicente, Y. Liu, M. J. Arellano-Jimenez, Z. Peng, T. Wang, Y. Li, B. I. Yakobson, S.-H. Wei, M. J. Yacaman and J. M. Tour, *Advanced materials*, 2016, **28**, 1427-1432.
18. Y. Cheng, S. Lu, F. Liao, L. Liu, Y. Li and M. Shao, *Advanced Functional Materials*, 2017, **27**, 1700359.